UV-curable coatings for energy harvesting applications: Current state-of-the-art and future perspectives

MNE 23 (2024) 100266

Contents lists available at ScienceDirect

Micro and Nano Engineering

journal homepage: www.sciencedirect.com/journal/micro-and-nano-engineering

Review paper

UV-curable coatings for energy harvesting applications: Current state-of-the-art and future perspectives

Donatella Duraccio [a], Pier Paolo Capra [b], Giulio Malucelli [c,*]

[a] Institute of Sciences and Technologies for Sustainable Energy and Mobility, National Council of Research, Strada delle Cacce 73, 10135 Torino, Italy
[b] National Institute of Metrological Research, Strada delle Cacce, 91, 10135, Torino, Italy
[c] Politecnico di Torino, Department of Applied Science and Technology, Viale T. Michel 5, 15121 Alessandria, Italy

ARTICLE INFO

Keywords:
UV curing
Coatings
Piezoelectric fillers
Energy harvesting
Additive manufacturing

ABSTRACT

Generally speaking, energy harvesting is an up-to-date technology that describes the possibility of capturing small amounts of energy (thermal, solar, or mechanical) from the surroundings and storing them as electrical energy for later uses when needed. Among the energy harvesting systems, the use of piezoelectric thin films and coatings is gaining increasing interest from both the academic and industrial communities, as these systems allow for the design and development of micro- and nano-scale devices, thanks to the possibility of being micro-machined and to the added functionality offered by the electromechanical coupling. These peculiarities justify their use for different applications, ranging from high energy density harvesters to high sensitivity sensors, and even low power consumption and large displacement actuators. Further, the current focus of the research on piezoelectric energy harvesting coatings is shifting from fully inorganic to hybrid organic-inorganic (i.e., composite) systems, as the latter can offer higher flexibility (i.e., lower stiffness), making them more sensitive to small vibrations and therefore suitable for these specific harvesting conditions. In this regard, photoinduced polymerization (the so-called "UV-curing") has become a suitable and reliable technique for the manufacturing of piezoelectric composite systems, as it is a solvent-free approach that allows for transforming a liquid mixture of monomers/oligomers into a solid 3D network in a few seconds, with a very limited energy consumption and a very high conversion. Besides, as the UV-curing process is very fast, the dispersed ceramic piezoelectric phase is not prone to settle down in the liquid resin, hence ensuring its homogeneous distribution within the polymer network after curing and better piezoelectric performance. The present review aims to provide the reader with an up-to-date overview of UV-curable coatings for piezoelectric energy harvesting purposes, highlighting their potential and piezoelectric features; further, some perspectives about possible future developments will be proposed.

1. Introduction

Piezoelectric materials are responsible for the efficient conversion of mechanical vibrations into electrical energy (as it occurs in such devices as sensors or energy transducers); the opposite effect, i.e., the possibility of undergoing deformation upon the application of an electric field, makes these materials suitable for being employed as actuators [1,2]. This peculiarity was first assessed for selected crystalline materials (natural or synthetic) like tourmaline, quartz, and barium titanate, among others. Nowadays, there exists a plethora of piezoelectric materials with different properties and characteristics: in a general approach, it is possible to divide piezoelectric materials into three main classes, i.e., piezoceramics, piezopolymers, and polymer matrix-based piezocomposites. Piezoceramic materials (such as $PbZr_xTi_{12x}O_3$, $BaTiO_3$, ZnO, and GaN, among others) are the most preferred, as they exhibit high electro-mechanical coupling constants and energy conversion rates; however, their high stiffness and, therefore, brittleness, does not suggest their use as energy transducers when high mechanical stresses are applied [3,4]. Conversely, the high flexibility and ease of processing of such piezopolymers as PVDF makes them suitable for several uses, despite their quite low electro-mechanical coupling constants [5,6]. The limitations exhibited by these two classes of piezoelectric materials can somehow be overcome by using piezocomposites, which can combine the flexibility and ease of processing of the polymer matrix (that usually

* Corresponding author.
E-mail address: giulio.malucelli@polito.it (G. Malucelli).

https://doi.org/10.1016/j.mne.2024.100266
Received 20 March 2024; Received in revised form 15 May 2024; Accepted 25 May 2024
Available online 27 May 2024

does not possess piezoelectric features) with the piezoelectric character of the filler(s) embedded in [7–9].

Specifically referring to piezocomposites based on thermosetting polymer matrices, photoinduced polymerization (i.e., UV-curing) has been identified as a possible, robust method to produce these materials, thanks to several advantages [10–12]. In particular, UV-curing is a very fast process that allows for the conversion of a liquid monomeric/oligomeric mixture containing a suitable photoinitiator into a 3D solid network. The reaction usually does not require the use of other chemicals/solvents, hence strongly limiting the environmental pollution due to the release of Volatile Organic Compounds (VOC). Besides, compared with the classical thermal curing processes, the energy required for UV-curing reactions is very low and limited to the operation of the UV lamps. Further, specifically referring to the production of piezocomposite thick or thin systems, the piezoelectric filler(s) that are dispersed into the liquid resins do not have time to give phase separation, as the reaction is very fast, hence ensuring a very homogeneous distribution within the cured polymer [13]. Finally, it is possible to tailor the flexibility of the final piezocomposites by simply optimizing the formulation of the liquid resin system.

Despite the huge number of nice papers on UV-curing and UV-curable systems that were published so far [13–19] and apart from a few general reviews on UV-curable smart coatings [20,21], the scientific literature lacks review works specifically devoted to the description of the structure, morphology and performance of UV-curable piezoelectric composite systems, which can provide the reader with an overview of their potential, even envisaging possible industrial applications.

Based on all these considerations, the present work aims to summarize the research carried out so far on the design, preparation, and characterization of UV-curable piezoelectric composites, highlighting their potential and performances; further, some perspectives about the possible developments for the forthcoming years will be proposed.

2. A general overview of photopolymerizable coatings for energy harvesting applications

2.1. UV-curing mechanisms

Photocurable coatings for harvesting applications have been designed not only for enhancing the efficiency of various harvesting processes, such as solar energy harvesting or harvesting light for sensors and optical devices [22–26] but also as a possible substitute for thin and thick films of piezoelectric ceramics [27–29], which are usually brittle and cannot withstand dynamic loadings. The flexible UV-cured systems are also easy to integrate into devices and show improved device reliability, reduced size, and production costs [30,31]. Also, because of their wide variety of properties, dimensional precision, and fast process, photopolymerizable coatings are particularly suitable for additive manufacturing processes that are emerging technologies for producing energy harvesting materials [32].

A photopolymerizable coating for energy harvesting can be prepared by adding an active piezoelectric filler (generally composed of ceramic micro- and nano-particles or nanowires) as a dispersed phase to the photocurable system (Fig. 1), which can be photopolymerized exploiting free-radical or cationic mechanisms. The most employed radical UV-curable systems are based on acrylates, which comprise a wide range of monomers and oligomers and exhibit high reactivity.

Three basic components commonly compose the acrylic systems: i) the monomers, acting as reactive diluents for adjusting the viscosity of the system, ii) the functionalized oligomers or prepolymers that form the backbone of the polymer network, and iii) the photoinitiator that produces free radicals upon exposure to UV radiation [33].

Besides, very often the UV-curable recipe is integrated by the addition of micro- or nano-fillers, capable of enhancing some properties of the final cured system (such as its thermal or electrical conductivity, thermal stability, mechanical strength, physicochemical behavior, among others) [34–38]. In this case, it becomes crucial to select the proper photoinitiating system (photoinitiator + photosensitizer) to avoid detrimental interactions between the UV radiation and the embedded filler, which may lower the quantum efficiency of the photopolymerization process.

In the cationic curing, the initiation mechanism is the photoinduced release of a Brönsted acid, able to give rise to the formation of carbocationic propagating species. The polymer is then formed through the repetitive addition of monomers to the growing carbocationic chain [39].

The radical UV-curing represents an economic and fast curing method characterized by low emissions of volatile organic compounds (VOCs) [40] and is more commercially widespread with respect to the cationic photopolymerization. Indeed, the high sensitivity of the latter toward water makes more difficult its industrial application; then, compared to free-radical photopolymerization, cationic photopolymerization shows a remarkably lower kinetic rate. In addition, the conversion of the reactive groups is often incomplete, leading to the formation of somehow unstable UV-cured networks. Finally, the availability and tunability (in terms of T_g – glass transition temperature and therefore of flexibility of the resulting UV-cured systems) of monomers and oligomers suitable for cationic photopolymerization are quite limited, compared to the radical systems. However, cationic photopolymerization is finding increasing applications as it does not suffer from oxygen inhibition and can polymerize such monomers as oxiranes and vinyl ethers, which do not polymerize through a free radical

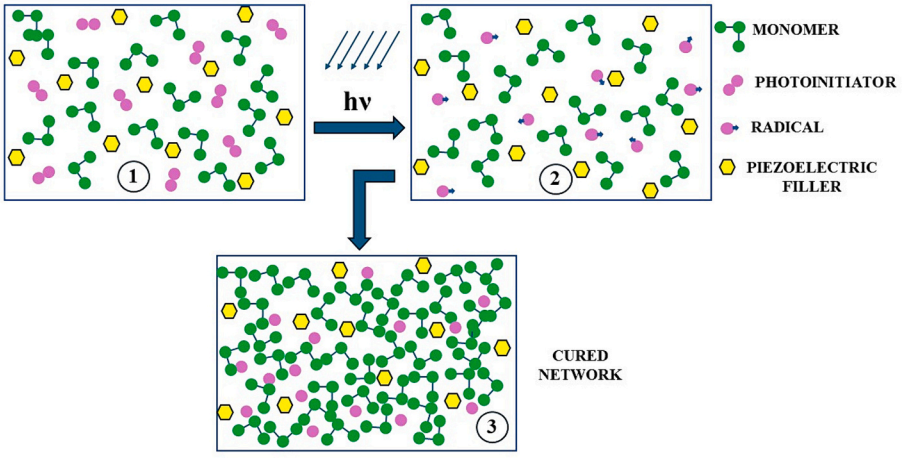

Fig. 1. Schematic representation of a UV-curing process.

mechanism [41]. In addition, cationic photopolymerization can continue also after the removal of the radiation source, if reactive species are still present in the systems. Moreover, the shrinkage of the polymers during cationic photo-curing is lower than in the free radical process, assuring good mechanical properties and adhesion to various substrates. These processes have been nicely reviewed in the scientific literature [39,42,43].

2.2. UV-curable coatings for energy harvesting: design and testing

The UV-cured energy harvesting systems are based on piezoelectric effects. The piezoelectric effect is a phenomenon where a material generates an electric charge in response to mechanical stress or deformation. Conversely, this material also undergoes mechanical deformation or strain when subjected to an electric field. This bidirectional coupling between mechanical and electrical properties forms the basis of piezoelectricity. More in detail, in the direct piezoelectric effect, a mechanical force is applied to a piezoelectric material causing a deformation or strain within the material's crystal lattice structure. This deformation disrupts the equilibrium of positive and negative charges within the material, resulting in the separation of electric charges along certain crystal planes. As a result, an electric polarization is induced within the material, creating an electric field, and generating a voltage across its surfaces. This effect is directly proportional to the applied mechanical stress and is reversible: in fact, the magnitude of the generated electric charge depends on the magnitude and direction of the applied force. In the converse piezoelectric effect, an external electric field is applied across the piezoelectric material, causing a displacement or mechanical deformation. This electric field exerts a force on the charged particles within the material, causing them to shift positions and resulting in a change in the material's dimensions. Again, the material experiences mechanical strain or deformation proportional to the strength and direction of the applied electric field; this effect is also reversible. [44,45] A schematic representation of this phenomenon is reported in Fig. 2.

Different ceramic powders were used as piezoelectric components for the preparation of UV-curable systems. The most commonly employed include lead zirconate titanate (PZT), barium titanate (BTO), and zinc oxide (ZnO). Despite its usefulness, PZT also poses environmental concerns due to the lead content, which can have adverse effects if not properly managed during manufacturing and disposal. Efforts are ongoing to develop lead-free alternatives with similar or improved properties [46]. $BaTiO_3$ (BTO) has a very high piezoelectric coefficient and dielectric constant [47]. However, durability and flexibility represent drawbacks for its application. ZnO is a versatile material with biologically safe piezoelectric semiconductor properties and occurring in a wide range of micro to nano-structured forms. It is inexpensiveness and possesses good chemical stability in air atmosphere [48].

Also, as organic fillers, polyvinylidene fluoride (PVDF) and cellulose were employed for the preparation of all-polymer-based piezoelectric photocurable resin. PVDF is, indeed, a popular material for piezoelectric applications. It is characterized by high flexibility, chemical inertness toward many chemicals, resistance to moisture and UV radiation; further, it can be processed into various forms and possesses high sensitivity, biocompatibility, and inexpensiveness [49]. More recently, cellulose has been considered in the field, although the piezoelectricity of wood was known from 1950s [50]. However, its piezoelectric constant is small, mainly due to the heterogeneous distribution of crystals and the relatively low degree of crystallinity of cellulose in the lignocellulose matrix. Given their native crystalline nature, cellulose nanocrystals (CNC) have been reasonably studied as potential materials for energy harvesting purposes [51,52].

The characterization of the piezoelectric performance of coatings can be obtained using a piezo-force microscope, a piezometer, and an oscilloscope. Piezo force microscopy (PFM), a type of scanning probe technique, has been demonstrated to be a reliable and useful characterization method for assessing the piezoelectric response of materials at small length scales. Although this method is based on standard contact mode atomic force microscopy (AFM), it can also be employed for applying an alternating voltage to the piezoelectric system. While the PFM image offers information on the local polarization orientation, the PFM amplitude data provide information on the size of the local electromechanical couple, from which the piezoelectric coefficient d_{33}, i.e., the charge per unit force in the polarization direction [53], is obtained. Another advantage of this method is that the active coating can be tested without any further treatment, whereas with the piezometer and the oscilloscope, electrodes need to be deposited on both sides of the active substrate to collect the generated charges. Among the most common methods, both Radio-frequency (RF) sputtering and the brushing method are often utilized. The RF sputtering, which is a physical vapor deposition (PVD) technique, operates on the principle of momentum transfer from high-energy ions to atoms in a target material, causing

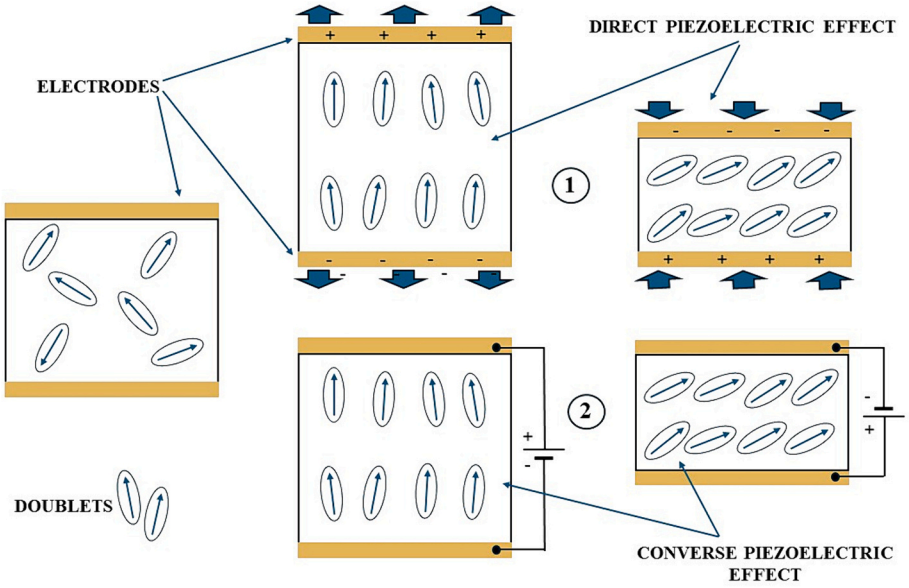

Fig. 2. Scheme of the direct (1) and indirect (2) piezoelectric effect.

them to be ejected (i.e., sputtered) from the target surface. These ejected atoms then condense onto a substrate, forming a thin film. [54] In the brushing method, a thin layer of material is deposited by a brush. This method is particularly common in small-scale applications or areas, where spray application may not be feasible [55].

In a piezometer, the sample, on which electrodes have been deposited, is clamped in the experimental apparatus (Fig. 3) between two electrical contacts (2) when they apply a compressive force F perpendicular to the surface of the sample (1). The arm (3) can be vertically moved, varying the force applied to the sample. The load cell (4) measures the total applied force. The piezoelectric voltage generated by the sample can be measured through the two terminals arranged laterally to the piezometer (5) by connecting to a digital multimeter suitable for measuring small signals. Processing the electrical signal emitted from the sample allows for a direct reading of the material d_{33} because of an integrated reference. The electric signals acquired by the sample under test are compared with a built-in reference and processed to give a direct reading of the d_{33} coefficient. Sometimes, the piezoelectric voltage constant (g_{33}), i.e., the ratio between d_{33} and ε, where ε is the material dielectric constant, can be found in the literature [56]. This methodology is sometimes referred to as the "Berlincourt" or "quasi-static" technique [57]. When compared to other static techniques, a piezometer offers better resolution and reliability and may be used with a wide range of sample geometries providing a quick, practical, and precise reading in a few seconds.

The oscilloscope is a versatile electronic test instrument used to observe and measure the voltage signals of electrical circuits. It displays the waveform of electrical signals in real-time, allowing engineers, technicians, and scientists to analyze various characteristics of the signals. It can be easily connected to a generator and a shaker actuator, which reproduce a mechanical solicitation for measuring the piezoelectric characteristics of a thin film/coating [55,58,59]. An example of the block diagram of the measurement system is shown in Fig. 4. Briefly, the mechanical excitation of the polymer layer is performed using a shaker (1), which generates motion along the axis identified by the output pin. This motion is modulated by an electrical signal generated by the oscillator inside the lock-in amplifier (5) and amplified through the buffer 2. The samples under test (SUT) are kept at the end of the shaker's output pin, as indicated in detail 7. Immediately below and connected to the SUT, force, and acceleration sensors (signals S2) are positioned, which are amplified by the multi-channel unit 3 and displayed and recorded by the oscilloscope (4, channel n.3).

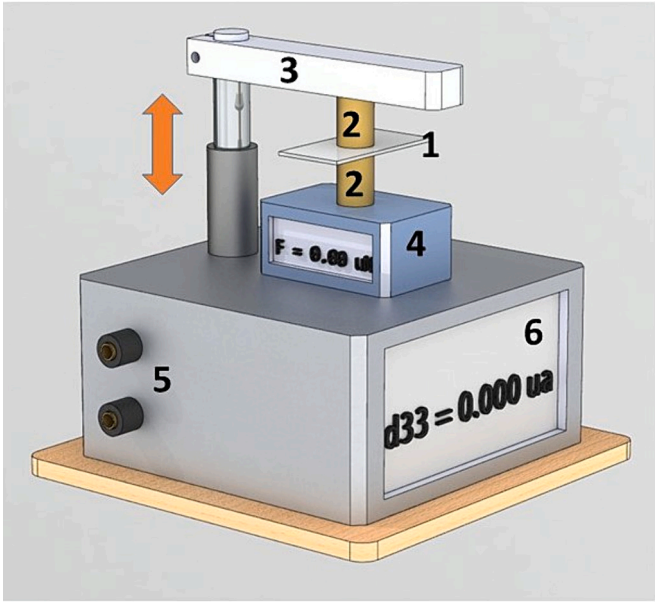

Fig. 3. Schematic representation of a commercial piezometer for measuring d_{33} piezoelectric coefficient.

The excitation signal produced by the SUT (signal S1) is detected by the lock-in amplifier, acquired, and displayed on channel n.2 of the oscilloscope.

The system is fully automated, and a computer controls the excitation of the devices, modulation waveforms, and signal acquisition.

Often, to activate or maximize the piezoelectric properties of the material a poling process is required. The poling process allows for the alignment of the electric dipoles within the material, which induces a permanent polarization. Proper control and optimization of the poling process are essential to ensure the reliability and performance of piezoelectric devices.

Briefly, the prepared material is placed in a high electric field generated by applying a voltage across the electrodes attached to the surfaces of the piezoelectric material. The magnitude and duration of the electric field are carefully controlled based on the material's properties and desired polarization [60]. A schematic representation of the poling is reported in Fig. 5.

2.3. UV-curable piezoelectric coatings for additive manufacturing processes

Additive manufacturing, as a cutting-edge manufacturing method, offers numerous advantages for the fabrication of piezoelectric materials, including the ability to create complex geometries, customization, material efficiency, reduced lead times, integration of multiple materials, and miniaturization. Different reviews summarize the advantages of additive manufacturing technology and its technical impact on the production of piezoelectric materials [21,61].

Stereolithography (SLA) is a 3D printing technology that exploits UV-curable systems to create three-dimensional objects in a layer-by-layer manner. The process begins with the creation of a 3D digital model, using computer-aided design (CAD) software, which defines the geometry of the object to be printed. The digital model is sliced into thin horizontal layers using slicing software. Each layer is translated into a series of two-dimensional cross-sections that the printer will use to construct the object. The SLA printer consists of a build platform and a resin vat filled with UV curable resin and the piezoelectric filler. The build platform is lowered into the resin vat, submerging it just below the surface of the liquid resin. A UV laser or light source is directed onto the surface of the liquid resin. The UV radiation is precisely controlled by mirrors or galvanometers based on the digital model's sliced layers. Wherever the UV light strikes the resin, it initiates a photopolymerization reaction, accounting for the solidification of the resin and the formation of a thin layer of the object. After solidifying one layer, the build platform moves down (or the resin vat moves up) by a distance equal to the height of one layer (Fig. 6). A recoating system then spreads a thin layer of fresh liquid resin over the solidified layer, preparing it for the next layer to be printed. This process of exposing, solidifying, and moving the build platform is repeated layer by layer until the entire object is built up. After processing, the printed object may undergo cleaning in a solvent to remove excess uncured resin and often it is further cured under UV radiation (provided by a UV oven) to ensure complete polymerization and enhance its mechanical properties [62].

With SLA, practically any form can be created and the advantages of using this technique are rapid production, high fidelity, accuracy, and high resolutions [63]. However, the particle loading is restricted because of the increase in viscosity and transparency, which prevent the radiation from penetrating and curing the system completely.

Kim et al. [63] used a process called dynamic optical projection stereolithography (DOPsL) [64] to achieve higher throughput and resolutions of 3D printed piezoelectric materials as compact sensors and energy scavengers. They prepared composites by loading chemically modified BTO (~85 nm) nanoparticles into the photocurable resin, namely polyethylene glycol diacrylate (PGEDA). Different loadings of

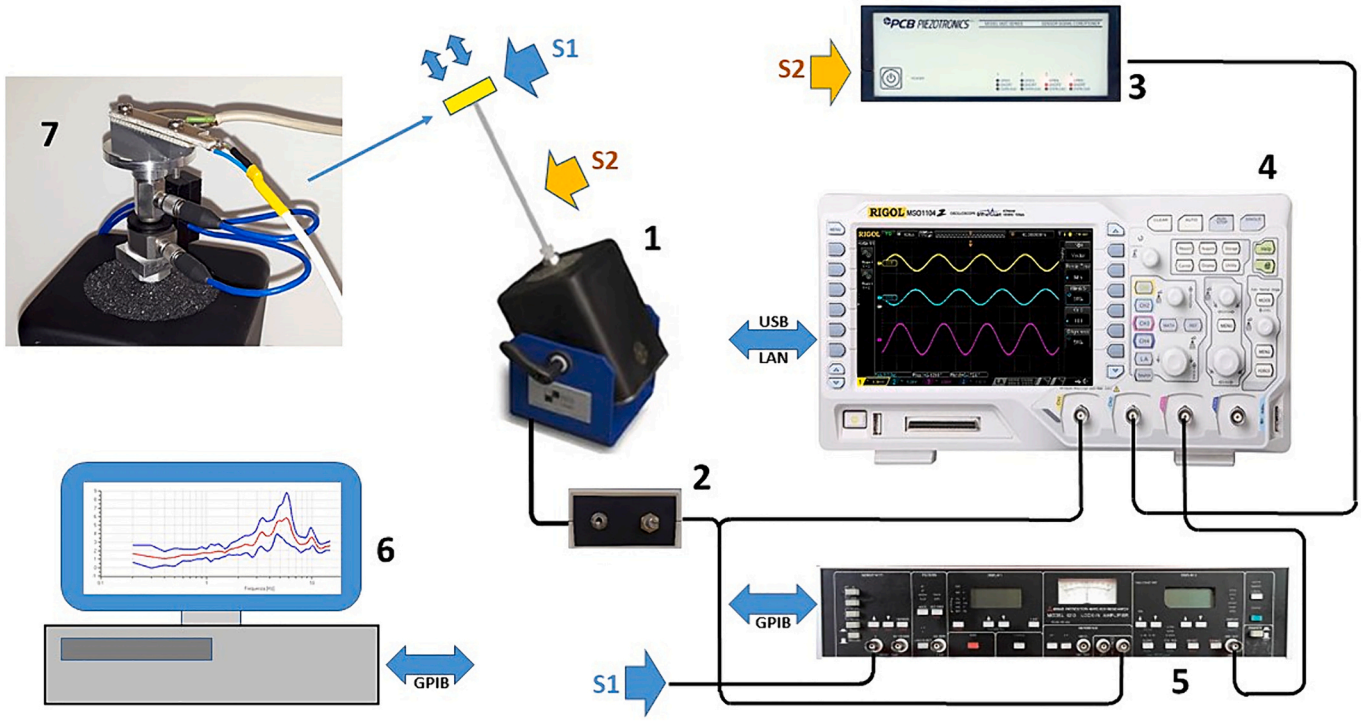

Fig. 4. 1) Shaker; 2) audio-frequency amplifier; 3) accelerometer amplifier 4) oscilloscope; 5) lock-in amplifier; 6) computer control, and 7) sample holder.

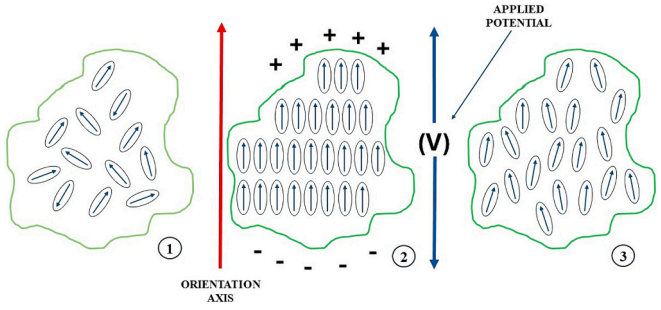

Fig. 5. Schematic representation of a poling process. (1) Randomly aligned dipole domains in a piezoelectric material; (2) Aligned domains during poling; (3) Permanent domains after poling.

BTO were used, namely 1, 5, and 10 wt%. Dots, square, and honeycomb arrays were obtained, as reported in Fig. 7. Further, the use of 3-trimethoxysilylpropyl methacrylate (TMSPM) as a crosslinking agent able to covalently bond the polymer chains to the BTO particles enhanced the mechanical-to-electrical energy conversion process by transferring the stress applied to the organic phase to the BTO crystals, in turn causing a large increase in the piezoelectric coefficient. More in detail, after poling (120 MVm^{-1}), the composites embedding 10 wt% BTO nanoparticles showed a piezoelectric coefficient (d_{33}) of ~40 pC/N, 10 times higher than the composites containing unmodified BTO and 2 times higher than the composites containing unmodified BTO nanoparticles and carbon nanotubes used with the aim to increase the stress transfer.

Chen et al. [65] reported the development of an all-polymer-based piezoelectric photocurable resin by projection micro stereolithography (PμSL). More in detail, they dispersed PVDF powders (from 15 to 50 wt% loading) into 1,6-hexanediol diacrylate (HDDA), aiming to increase the system flowability, obtaining low piezoelectric properties at low PVDF concentrations. Conversely, high filler concentrations caused problems during processing because of the very high viscosities of the system. The films were poled between 1.33 and 12 MVm^{-1} and the optimized film

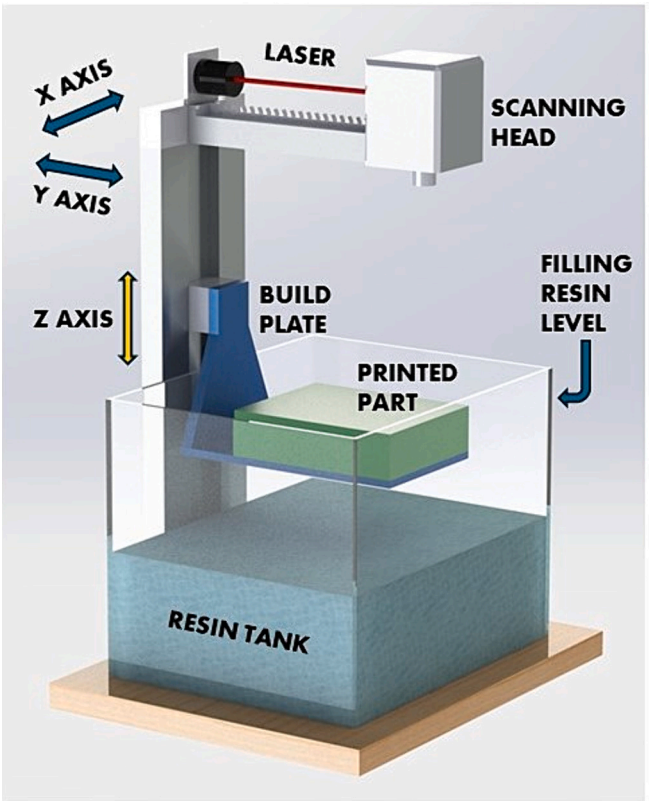

Fig. 6. Schematic representation of Stereolithography. Selective resin polymerization occurs through exposure to laser radiation and the xy movement of the print head, while simultaneously moving the object under construction along the z-axis, achieving accuracies on the order of 0.1 mm.

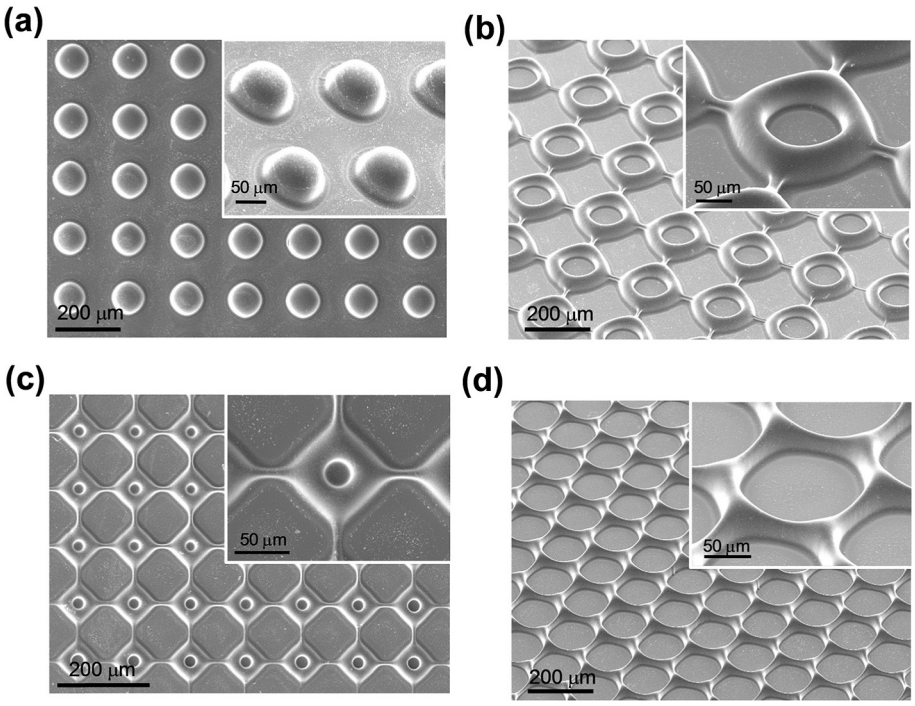

Fig. 7. Piezoelectric microstructures printed using DOPsL including (a) a dot array, (b, c) square arrays with different sized void spaces, and (d) a honeycomb array. Reprinted with permission from Ref. [63]. Copyright 2014, American Chemical Society.

containing 35 wt% PVDF powder resulted in an increased g_{33} from 19 to 105 $mVmN^{-1}$ (+450%, Fig. 8), which is in the same range as the pure PVDF film (140–330 $mVmN^{-1}$) [66].

Zhou et al. [67] used photocurable elastomers (i.e., epoxy aliphatic acrylate (EAA) and aliphatic urethane diacrylate (AUD)) in equal amounts and 15 wt% of BTO to give rise, for the first time, to a 3D printable ink and a printed stretchy film to be used for energy harvesting applications. The films had a maximum strain of 434% and a current density of 0.20 $\mu A/cm^2$, an output voltage of 0.29 V, and a power density of 57 nW/cm^2.

More recently, Wang et al. [68] produced piezoelectric composites via photocuring 3D printing and investigated their properties through both experimental and theoretical means, demonstrating their potential as energy harvesters. Different shapes were obtained such as thin round-hole, dumbbell, and lattice structures. For the preparation of the slurry, they used 40–60 wt% of PZT as piezoelectric micrometric powder and a photocurable resin composed of hydroxyethyl methacrylate (HEMA), ethoxylated trimethylolpropane triacrylate (ETPTA). To reduce the weak interface bonding between the organic and inorganic phases, PZT ceramic powders were grafted with a silane coupling agent that in turn resulted in a covalently bonded link between PTZ particles and the matrix.

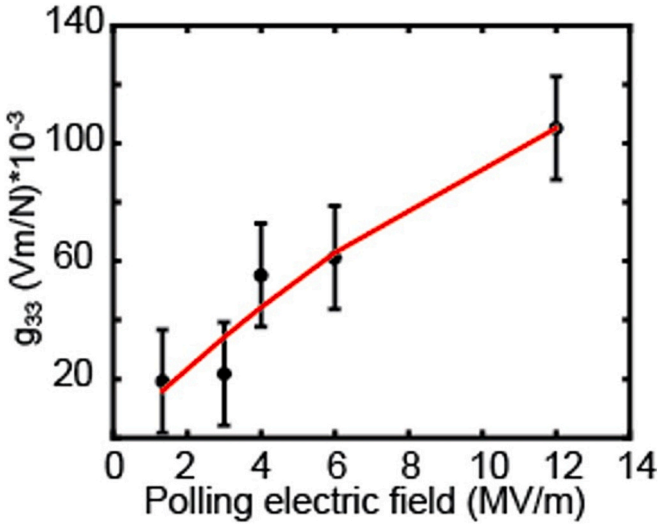

Fig. 8. Calculated g_{33} coefficient for 3D printed PVDF sensors versus poling electric field. Reprinted from Ref. [65] under CC-BY license.

By a simulation analysis [69] it was demonstrated that the piezoelectric constant of the composites is a function of both the elastic modulus of the interfacial layers and the particle volume fraction. Also, it was found that the silane modification led to an increase in the elastic modulus of the interface layers and in the piezoelectric constants up to 37 pC/N, also according to the simulation results. In a complementary work, Wang et al. [70] used oleic acid-grafted PZT particles instead of silane for the preparation of a stable slurry to be printed by SLA. The results revealed that when 72 wt% of grafted ceramic particles were used, the piezoelectric voltage constant was 220.2 $\times$ 10^{-3} $Vm{\cdot}N^{-1}$. **Figs. 9** and **10** report the relationship between the concentration of the coupling agents (i.e., silane and oleic acid, respectively) and the piezoelectric constant of piezoelectric composites, evidencing the importance of maximizing the interface bonding between organic and inorganic phases, which helps the mechanical-to-electrical energy conversion process.

2.4. UV-curable thin free-standing films and coatings

ZnO and BTO micro/nano particles were mixed with UV-curable resins for the fabrication by photo-lithography of piezoelectric micro-electromechanical-systems (MEMS) and nano-electromechanical-systems (NEMS) for energy harvesting applications [71–74]. In these works, an epoxy-based, transparent, negative photoresist, developed by IBM [75] was used as a UV-curable system, coded as SU-8. Prashanthi et al. [71] incorporated 20 wt% of ZnO nanoparticles into SU-8 that was spin-coated on a Ti/Au deposited Si substrate, followed by a thermal treatment to evaporate the solvent. Interestingly, the film showed a d_{33} coefficient of 6.2 pmV^{-1}, similar to that found for bulk ZnO [76]. In this

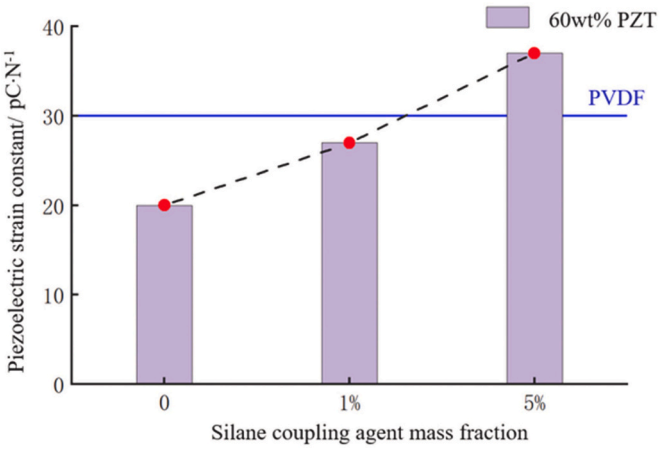

Fig. 9. Comparison of the effect of silane concentration on the piezoelectric properties of piezoelectric composites. Reprinted with permission from Ref. [68]. Copyright 2022, Elsevier.

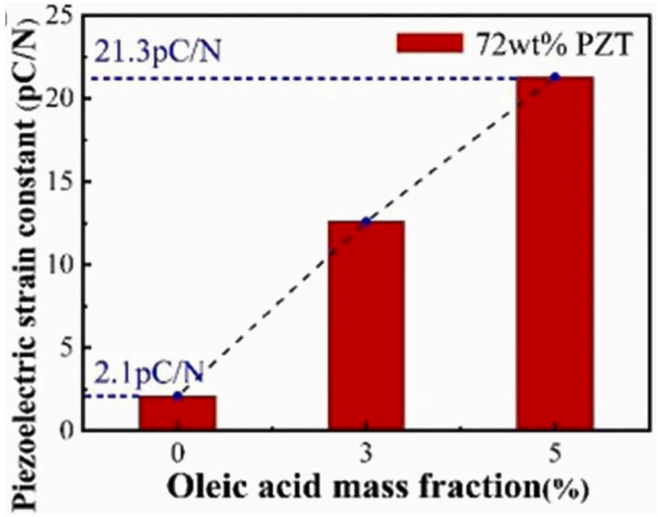

Fig. 10. Comparison of the effect of oleic acid concentration on piezoelectric properties of piezoelectric composites. Reprinted with permission from Ref. [70]. Copyright 2023, Elsevier.

work, it was also shown that the presence of 20 wt% ZnO did not modify the photosensitivity and optical transparency of the resin, demonstrating its feasibility for fabricating MEMS by photolithography. Pursuing this research, Kandpal et al. [72] investigated the physical characteristics of SU-8/ZnO nanocomposite thin films at increasing ZnO loadings (namely, from 5 to 20 wt%). In particular, they demonstrated that it was possible to fabricate a micro-cantilever structure at any composition by photolithography (Fig. 11). Moreover, they found that the resonant frequency response of the piezoelectric device, ranging between 15 and 23 pm V^{-1}, was correlated with the stiffness of the epoxy nanocomposites that in turn was associated with ZnO concentration. Similarly, Krishna et al. [73] reported a structural and mechanical analysis of SU-8/ZnO nanocomposites varying the amount of ZnO from 0 to 25 wt%. They verified that the optical transparency of nanocomposites to UV radiation was maintained up to 20 wt% of ZnO. At higher concentrations (i.e., 25 wt%), the nanocomposites could not be patterned. In another work, both SU-8/ZnO and SU-8/BTO nanocomposite thin films were fabricated for mechanical energy harvesting applications [74]. Optimized results with good piezoelectric response and UV transmittance were obtained for nanocomposites containing 15 wt% of ZnO and 20 wt% of BTO. Open circuit voltages of 570 mV and

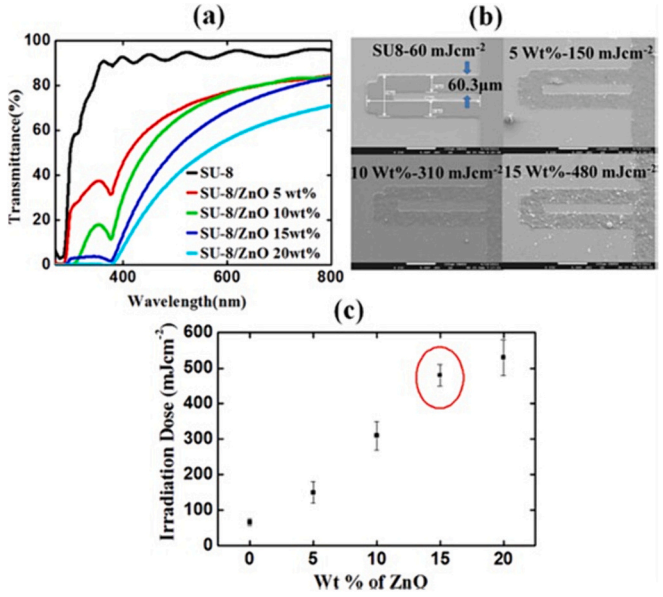

Fig. 11. Irradiation dose needed for photo-lithography of the nanocomposite films as a function of ZnO wt%. (a) Transmission characteristics of the nanocomposites; (b) SEM images of the patterned structures; (c) Optimized doses. Reprinted with permission from Ref. [72]. Copyright 2012, American Institute of Physics.

780 mV were obtained for SU-8/ZnO and SU-8/BTO nanocomposite respectively when they were stressed by regular finger pressing. The voltages even increased when the nanocomposites were employed as harvesters combining piezoelectric triboelectric and transduction mechanisms.

Using a simpler approach, Malucelli et al. prepared UV-cured composite films based on bis-phenol A ethoxylate diacrylate (Ebecryl 150) filled with different ZnO objects, differing as far as their morphologies are concerned (i.e., long needles, spherical nanoparticles, bipyramidal and flower-like morphologies) [28]; these ZnO objects were incorporated at 4 wt% loading into the acrylic matrix (Fig. 12). Films were obtained by coating the dispersion on a glass slide and exposing it to UV radiation; the thickness of the resulting films was about 150 μm.

Regardless of the low ZnO concentration, all the UV-cured composite films showed intriguing piezoelectric responses that were measured at various accelerations applied to the films and expressed in terms of root mean square (RMS) open circuit voltage. In particular, the films with flower-like morphologies showed the best piezoelectric performance at the resonance frequency and at 150 Hz, reaching a maximum RMS voltage of 0.914 mV when 5.79 g of acceleration was applied. Conversely, the lowest RMS voltage values were found for the film containing needle-like ZnO. This finding was interpreted considering the direction of the (002) crystallographic planes in needle-like ZnO, which was perpendicular to the applied mechanical solicitation and thus less effective from a piezoelectric point of view.

Pursuing this research, Duraccio et al. prepared UV-cured composite films made of the same acrylic resin filled with flower-like and needle-like zinc oxide (i.e., corresponding to the highest and lowest piezoelectric performances) in different amounts (i.e., 4, 10, and 20 wt%). This way it was possible to assess the influence of the filler concentration on the piezoelectric response of UV-curable films at a lower frequency range (namely, from 1 to 100 Hz), corresponding to the environmental harvesting conditions [55]. The results showed that the piezoelectric response generated by the polymer composite films was very good at 19 Hz and was a function of the applied acceleration. In detail, the RMS output voltages achieved at 5 g were 4.94 and 1.85 mV for the composite films containing 20 wt% of flower-like and needle-like ZnO, respectively (Fig. 13). Interestingly, the decrease in the storage modulus of the

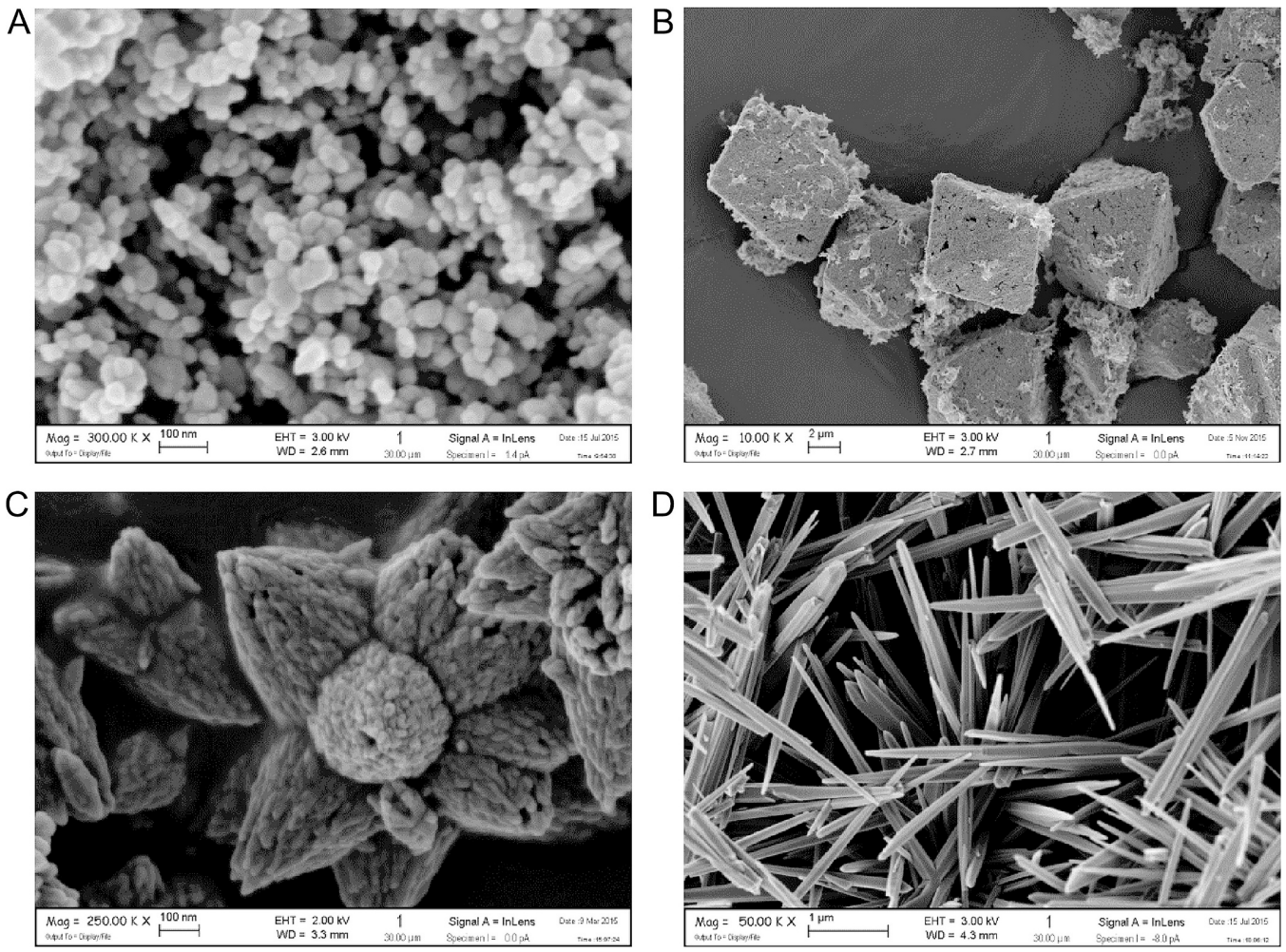

Fig. 12. Micrographs of different ZnO morphologies obtained by sol-gel method. (A) nanoparticle; (B) bipyramidal; (C) flower-like morphology; (D) long needles. Reprinted with permission from Ref. [28]. Copyright 2017, Elsevier.

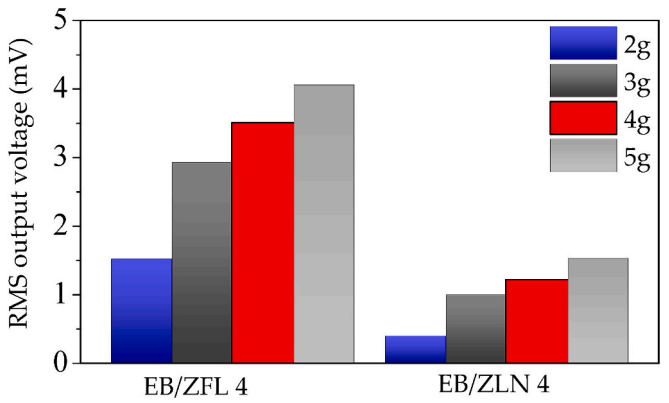

Fig. 13. RMS output voltage values produced by composites containing 4 wt% of ZnO (flower-like (ZFL) and needle (ZLN) structures) at the frequency of 19 Hz and different acceleration values (namely, 2, 3, 4, and 5 g). Reprinted from Ref. [55] under CC-BY license.

composites with high ZnO loading, rather than the filler's dispersion or the amount of ZnO particles on the surface, was interpreted as the main reason for the RMS output voltage rise that was not proportional to the filler loading.

In another work, Signore et al. [29,77] studied the piezoelectric properties of UV-curable systems containing cellulose nanocrystals (CNCs), alone or in combination with different ZnO morphologies, embedded in Ebecryl 150. The presence of cellulose nanocrystals showed a detrimental effect on the piezoelectric properties of the composite films as compared with ZnO, due to the lower crystallinity of cellulose nanocrystals, as well as their worse interfacial adhesion with the polymer matrix. The integration of a powder vapor deposited AlN layer onto the top surface of the beam and the anchoring of a proof mass on the beam tip were also assessed, aiming to enhance the nanocomposite piezoelectric responses.

In particular, when ZnO flower-like morphologies were used, the nitride layer raised the RMS voltage from 1.0 to 3.9 mV. In fact, the addition of ZnO to the acrylic matrix promoted an ordered structural arrangement of the formed AlN layer, as demonstrated by XRD studies, which improved the resultant piezoelectricity. For the AlN-coated system with ZnO flower-like morphologies, the output voltage increased even more with the insertion of the proof mass, reaching 4.5 mV.

Finally, PTZ was also used as a powder for the preparation of piezoelectric coatings. In particular,

Payo et al. used a water-based acrylic polymer containing some additives (not specified) to achieve a viable coating [78]. The PTZ piezoelectric/polymer weight ratio was set at 3:2. The coating needed to be polarized with a high electric field of 5 kV mm^{-1} prior to use. After analyzing the collected energy as a function of sine vibration testing from 1 to 15 Hz, the authors obtained ≈60 nJ cm^{-2} for a vibration frequency of 15 Hz and a strain amplitude of 316 µm m^{-1} (test duration: 40 s).

Table 1
Recent advances in UV-curable piezoelectric coatings.

Type of UV-curable resin	Type of piezoelectric filler	Main outcomes	Ref.
PEGDA	BTO	• d_{33} of about 40 pCN^{-1} measured for the composites embedding 10 wt% filler	[63]
HDDA	PVDF	• g_{33} increased up to 105 $mVmN^{-1}$ in the presence of 35 wt% PVDF powder	[65]
EAA/AUD	BTO	• 0.20 μAcm^{-2} current density in the presence of 15 wt% BTO • 0.29 V output voltage in the presence of 15 wt% BTO • 57 $nWcm^{-2}$ power density in the presence of 15 wt% BTO	[67]
HEMA/ETPTA	PZT (silanized)	• g_{33} of 167.2 $mVmN^{-1}$ in the presence of 60 wt% PZT	[68]
Mixture of acrylic resins	PZT (modified with oleic acid)	• g_{33} of 220.2 $mVmN^{-1}$ in the presence of 72 wt% PZT	[70]
SU8	ZnO nanoparticles	• 0.025 μW output power in the presence of 20 wt% ZnO	[71]
SU8	ZnO nanoparticles	• d_{33} of about 23 pCN^{-1} measured for the composites embedding 20 wt% filler	[72]
SU8	ZnO nanoparticles	• the resulting UV-cured coatings can be microfabricated using photolithography	[73]
SU8	ZnO nanoparticles or BTO	• 570 mV open circuit voltage for the coatings embedding 15 wt% ZnO • 780 mV open circuit voltage for the coatings embedding 20 wt% BTO	[74]
Ebecryl 150	ZnO (different morphologies)	• 0.914 mV maximum RMS output voltage at resonance frequency for 4 wt% flower-like ZnO	[28]
Ebecryl 150	ZnO (different morphologies)	• 4.94 mV maximum RMS output voltage at 19 Hz frequency and 5 g acceleration for 20 wt% flower-like ZnO • 1.85 mV maximum RMS output voltage at 19 Hz frequency and 5 g acceleration for 20 wt% ZnO needles	[55]
Ebecryl 150	ZnO + CNC	• 2.4 mV maximum RMS output voltage at resonance frequency and 10 g acceleration for the coating embedding 2 wt% flower-like ZnO and 2 wt% CNC • 3.9 mV maximum RMS output voltage at resonance frequency and 10 g acceleration in the presence of a further AlN layer (thickness: 600 nm)	[29,77]
Waterborne acrylic resin	PZT	• about 60 $nJcm^{-2}$ collected energy as a function of sine vibration at 15 Hz frequency	[78]

Table 1 summarizes the main research outcomes described in this review work.

3. Conclusions and future perspectives

This work has summarized the current state-of-the-art related to the use of UV-curing as a fast, robust, reliable, and effective strategy for obtaining composite coatings with interesting piezoelectric features. Indeed, the dispersion of the piezoelectric filler(s) into the UV-curable liquid resin is usually very easy and allows for the obtainment of coatings that exhibit acceptable piezoelectric features even when the filler loading is not very high, taking advantage of its homogeneous distribution within the 3D polymer network. Besides, exploiting UV-curing in Additive Manufacturing processes paves the way toward a significant upscaling for the industrial production of piezoelectric devices with high electro-mechanical coupling coefficients that are necessary for enhancing the performances of energy harvesting coatings. In addition, the possibility of incorporating different piezoelectric fillers into various UV-curable resin systems and at different filler loadings allows for the customization of the obtained coatings in terms of flexibility, mechanical strength, piezoelectric features, and resistance to harsh vibrations and shocks, among others.

Despite all these very promising characteristics, there are still some limitations that make UV-curable piezoelectric coatings not so currently widely employed in the world of energy harvesting. First, particularly at high loadings, the homogeneous distribution of the piezoelectric filler(s) within the UV-cured polymer matrix is not always easy to control and maintain, thus lowering the piezoelectric performances of the final coatings: using selected coupling agents could ameliorate the filler dispersion and the overall piezoelectric outcomes.

The current piezoelectric coatings are often based on the incorporation of micron-sized piezoelectric fillers: downsizing the filler to the nanoscale could represent a further implementation if a homogeneous dispersion of the nanofiller is maintained, avoiding its reaggregation. Finally, the design and development of efficient electronic circuitries for energy harvesters still can be a limitation, even when the piezoelectric coatings are well implemented.

It is likely to be expected that, thanks to continuous technological development, all these issues can be at least partially resolved in the forthcoming years, leading to a more profitable use of these piezoelectric systems.

Declaration of competing interest

The authors declare that they have no known competing financial interests or personal relationships that could have appeared to influence the work reported in this paper.

Data availability

Data will be made available on request.

References

[1] M.C. Sekhar, E. Veena, N.S. Kumar, K.C.B. Naidu, A. Mallikarjuna, D.B. Basha, A review on piezoelectric materials and their applications, Cryst. Res. Technol. 58 (2023) 2200130.
[2] M. Safaei, H.A. Sodano, S.R. Anton, A review of energy harvesting using piezoelectric materials: state-of-the-art a decade later (2008–2018), Smart Mater. Struct. 28 (2019) 113001.
[3] H.S. Kim, J.-H. Kim, J. Kim, A review of piezoelectric energy harvesting based on vibration, Int. J. Precis. Eng. Manuf. 12 (2011) 1129–1141.
[4] S.P. Beeby, M.J. Tudor, N.M. White, Energy harvesting vibration sources for microsystems applications, Meas. Sci. Technol. 17 (2006) R175–R195.
[5] M. Smith, S. Kar-Narayan, Piezoelectric polymers: theory, challenges and opportunities, Int. Mater. Rev. 67 (2022) 65–88.
[6] S. Crossley, R.A. Whiter, S. Kar-Narayan, Polymer-based nanopiezoelectric generators for energy harvesting applications, Mater. Sci. Technol. 30 (2014) 1613–1624.
[7] S. Mishra, L. Unnikrishnan, S. Kumar Nayak, S. Mohanty, Advances in piezoelectric polymer composites for energy harvesting applications: a systematic review, Macromol. Mater. Eng. 304 (2019) 1800463.
[8] Z. Wu, Z. Yang, J. Zhang, X. Qu, Fabrication and characterization of the piezoelectric ceramic–polymer composites, Appl. Ceram. Technol. 13 (2016) 690–696.
[9] P. Kabakov, T. Kim, Z. Cheng, X. Jiang, S. Zhang, The versatility of piezoelectric composites, Annu. Rev. Mater. Res. 53 (2023) 165–193.
[10] A. Sheel Wali, S. Kumar, D. Khan, A review on recent development and application of radiation curing, Mater. Today: Proc. 82 (2023) 68–74.
[11] R.S. Patil, J. Thomas, M. Patil, J. John, To shed light on the UV curable coating technology: current state of the art and perspectives, J. Compos. Sci. 7 (2023) 513.
[12] M.G. Collinson, M.P. Bower, T.J. Swait, C.P. Atkins, S.A. Hayes, B. Nuhiji, Novel composite curing methods for sustainable manufacture: a review, Compos. Part C: Open Access 9 (2022) 100293.

[13] F. Liu, A. Liu, W. Tao, Y. Yang, Preparation of UV curable organic/inorganic hybrid coatings - a review, Prog. Org. Coat. 145 (2020) 105685.
[14] P. Nguyen-Tri, T. Vuong Nguyen, Radically curable nano-based coatings, 2019, pp. 339–372.
[15] M. Sangermano, I. Roppolo, M. Messori, UV-cured functional coatings, in: A. Tiwari, A. Polykarpov (Eds.), Photocured Materials ch.7, The Royal Society of Chemistry, 2014, pp. 121–133.
[16] M.D. Soucek, X. Ren, UV-curable coating technologies (2014). UV-Curable Coating Technologies, in: A. Tiwari, A. Polykarpov (Eds.), Photocured Materials, The Royal Society of Chemistry, 2014, pp. 15–48, ch. 2.
[17] S. Bastani, M. Mohseni, UV-curable nanocomposite coatings and materials, in: Handbook of Nanoceramic and Nanocomposite Coatings and Materials, Butterworth-Heinemann, 2015, pp. 155–182.
[18] M. Sangermano, N. Razza, J.V. Crivello, Cationic UV-curing: technology and applications, Macromol. Mater. Eng. 299 (7) (2014) 775–793.
[19] A. Vitale, G. Trusiano, R. Bongiovanni, UV-curing of adhesives: a critical review, Rev. Adhesion Adhes. 5 (2) (2017) 105–161.
[20] C. Mendes-Felipe, T. Rodrigues-Marinho, J.L. Vilas, S. Lanceros-Mendez, UV curable nanocomposites with tailored dielectric response, Polymer 196 (2020) 122498.
[21] C. Mendes-Felipe, J. Oliveira, I. Etxebarria, J.L. Vilas-Vilela, S. Lanceros-Mendez, State-of-the-art and future challenges of UV curable polymer-based smart materials for printing technologies, Adv. Mater. Technol. 4 (3) (2019) 1800618.
[22] D. Pintossi, A. Colombo, M. Levi, C. Dragonetti, S. Turri, G. Griffini, UV-curable fluoropolymers crosslinked with functional fluorescent dyes: the way to multifunctional thin-film luminescent solar concentrators, J. Mater. Chem. A 5 (19) (2017) 9067–9075.
[23] R. Magazine, B. van Bochove, S. Borandeh, J. Seppälä, 3D inkjet-printing of photo-crosslinkable resins for microlens fabrication, Addit. Manuf. 50 (2022) 102534.
[24] J.S. Kim, G.S. Shim, D. Baek, J.H. Back, S.W. Jang, H.J. Kim, J.-S. Choi, J.S. Yeom, UV/UV step-curing of optically clear acrylate adhesives for mobile devices, Express Polym Lett 13 (9) (2019) 794–805.
[25] H.K. Kim, J.G. Kim, J.D. Cho, J.W. Hong, Optimization and characterization of UV-curable adhesives for optical communications by response surface methodology, Polym. Test. 22 (8) (2003) 899–906.
[26] F. Liu, A. Liu, W. Tao, Y. Yang, Preparation of UV curable organic/inorganic hybrid coatings-a review, Prog. Org. Coat. 145 (2020) 105685.
[27] N. Soin, T.H. Shah, S.C. Anand, J. Geng, W. Pornwannachai, P. Mandal, D. Reid, S. Sharma, R.L. Hadimani, D.V. Bayramol, E. Siores, Novel "3-D spacer" all fibre piezoelectric textiles for energy harvesting applications, Energy Environ. Sci. 7 (2014) 1670–1679.
[28] G. Malucelli, A. Fioravanti, L. Francioso, C. De Pascali, M.A. Signore, M.C. Carotta, A. Bonanno, D. Duraccio, Preparation and characterization of UV-cured composite films containing ZnO nanostructures: effect of filler geometric features on piezoelectric response, Prog. Org. Coat. 109 (2017) 45–54.
[29] M.A. Signore, C. De Pascali, D. Duraccio, G. Malucelli, A. Fioravanti, E. Melissano, M.C. Martucci, M. Masieri, P. Siciliano, L. Francioso, J. Appl. Polym. Sci. 138 (2021) e49731.
[30] S. Banerjee, K.A. Cook-Chennault, An investigation into the influence of electrically conductive particle size on electromechanical coupling and effective dielectric strain coefficients in three phase composite piezoelectric polymers, Compos. A: Appl. Sci. Manuf. 43 (2012) 1612.
[31] S. Mishra, L. Unnikrishnan, S.K. Nayak, S. Mohanty, Advances in piezoelectric polymer composites for energy harvesting applications: a systematic review, Macromol. Mater. Eng. 304 (2019) 1800463.
[32] A. Zhakeyev, P. Wang, L. Zhang, W. Shu, H. Wang, J. Xuan, Additive manufacturing: unlocking the evolution of energy materials, Adv. Sci. 4 (10) (2017) 1700187.
[33] A. Endruweit, M.S. Johnson, A.C. Long, Curing of composite components by ultraviolet radiation: a review, Polym. Compos. 27 (2006) 119.
[34] F.M. Uhl, D.C. Webster, S.P. Davuluri, S.C. Wong, UV curable epoxy acrylate–clay nanocomposites, Eur. Polym. J. 42 (10) (2006) 2596–2605.
[35] D. Işın, N. Kayaman-Apohan, A. Güngör, Preparation and characterization of UV-curable epoxy/silica nanocomposite coatings, Prog. Org. Coat. 65 (4) (2009) 477–483.
[36] N. Lü, X. Lü, X. Jin, C. Lü, Preparation and characterization of UV-curable ZnO/polymer nanocomposite films, Polym. Int. 56 (1) (2007) 138–143.
[37] M. Martin-Gallego, R. Verdejo, M.A. López-Manchado, M. Sangermano, Epoxy-graphene UV-cured nanocomposites, Polymer 52 (21) (2011) 4664–4669.
[38] P. Wang, J. Guo, H. Wang, Y. Zhang, J. Wei, Functionalized multi-walled carbon nanotubes filled ultraviolet curable resin nanocomposites and their applications for nanoimprint lithography, J. Phys. Chem. C 113 (19) (2009) 8118–8123.
[39] J.V. Crivello, Cationic polymerization — Iodonium and sulfonium salt photoinitiators, in: Initiators — Poly-Reactions — Optical Activity. Advances in Polymer Science vol. 62, Springer, Berlin, Heidelberg, 1984, https://doi.org/10.1007/BFb0024034.
[40] C. Decker, The use of UV irradiation in polymerization, Polym. Int. 45 (1998) 133.
[41] J. Ortyl, R. Popielarz, New photoinitiators for cationic polymerization, Polimery 57 (2012) 510.
[42] J.V. Crivello, Photoinitiated cationic polymerization, Annu. Rev. Mater. Sci. 13 (1) (1983) 173–190.
[43] A. Javadi, H.S. Mehr, M. Sobani, M.D. Soucek, Cure-on-command technology: a review of the current state of the art, Prog. Org. Coat. 100 (2016) 2–31.
[44] A. Erturk, D.J. Inman, Introduction to piezoelectric energy harvesting, in: Piezoelectric Energy (2011). Piezoelectric Energy Harvesting, John Wiley & Sons, 2011, p. 1.
[45] J. Nunes-Pereira, et al., Piezoelectric energy production, Comprehens. Energy Syst. 3e5 (2018) 380.
[46] S. Gupta, D. Maurya, Y. Yan, S. Priya, Development of KNN-based piezoelectric materials, in: S. Priya, S. Nahm (Eds.), Lead-Free Piezoelectrics, Springer, New York, 2012, pp. 89–119.
[47] B. Ertuğ, The overview of the electrical properties of barium titanate, Am. J. Eng. Results 2 (2013) 1–7.
[48] M.-Y. Choi, D. Choi, M.-J. Jin, I. Kim, S.-H.S.-W. Kim, J.-Y. Choi, S.Y. Lee, J.M. Kim, Mechanically powered transparent flexible charge-generating nanodevices with piezoelectric ZnO, Nanorods, Adv. Mater. 21 (2009) 2185.
[49] T. Someya, Y. Kato, T. Sekitani, S. Iba, Y. Kiyama, T. Sakurai, Piezoelectric polymer PVDF (polyvinylidene fluoride): a review of the recent literature, IEEE Trans. Ultrason. Ferroelectr. Freq. Control 3 (2010) 478–489.
[50] V.A. Bazhenov, Piezoelectric Properties of Woods, Consultants Bureau, New York, 1961.
[51] J. Kim, S. Yun, Z. Ounaies, Discovery of cellulose as a smart material, Macromolecules 39 (2006) 4202–4206.
[52] S. Yun, J.H. Kim, Y. Li, J. Kim, Alignment of cellulose chains of regenerated cellulose by corona poling and its piezoelectricity, J. Appl. Phys. 103 (2008) 083301.
[53] A.L. Kholkin, S.V. Kalinin, A. Roelofs, A. Gruverman, Review of ferroelectric domain imaging by piezoresponse force microscopy, in: Scanning Probe Microscopy, Springer, Berlin, 2007, pp. 173–214.
[54] C.M. Horwitz, Radio frequency sputtering—the significance of power input, J. Vac. Sci. Technol. A 1 (4) (1983) 1795–1800.
[55] D. Duraccio, P.P. Capra, A. Fioravanti, G. Malucelli, Influence of mechanical properties on the piezoelectric response of UV-cured composite films containing different ZnO morphologies, Polymers 15 (2023) 1159.
[56] S. Priya, H.-C. Song, Y. Zhou, R. Varghese, A. Chopra, S.-G. Kim, I. Kanno, L. Wu, D. S. Ha, J. Ryu, R.G. Polcawich, A review on piezoelectric energy harvesting: materials, methods, and circuits, Energy Harvest. Syst. 4 (2017) 3–39.
[57] M. Al Ahmad, A. Allataifeh, Electrical extraction of piezoelectric constants, Heliyon 4 (2018), 00910–15.
[58] R.B. Oliveira, L.M. Marques, G.P. Pires, P.T. Araújo, R.R.S. Vaz, A simple, compact and low-cost setup for dynamic piezoelectric measurements of thin films using an oscilloscope, Measurement 100 (2017) 133–137.
[59] N. Adão, P.M. Vilarinho, A.L. Kholkin, A.L. Costa, L.F. Vieira, Characterization of piezoelectric thin films by optical and electrical measurements, Sensors Actuators A Phys. 92 (2001) 359–364.
[60] J. Moulson, J.M. Herbert, Piezoelectric Ceramics: Principles and Applications, Institute of Physics Publishing, 2008.
[61] C. Chen, X. Wang, Y. Wang, D. Yang, F. Yao, W. Zhang, B. Wang, G.A. Sewvandi, D. Yang, D. Hu, Additive manufacturing of piezoelectric materials, Adv. Funct. Mater. 30 (2020) 2005141.
[62] S. Corbel, O. Dufaud, T. Roques-Carmes, in: P.J. Bártolo (Ed.), Stereolithography: Materials, Processes and Applications, Springer US, Boston, MA, 2011, p. 141.
[63] K. Kim, W. Zhu, X. Qu, C. Aaronson, W.R. McCall, S. Chen, D.J. Sirbuly, 3D optical printing of piezoelectric nanoparticle–polymer composite materials, ACS Nano 8 (2014) 9799.
[64] A.P. Zhang, X. Qu, P. Soman, K.C. Hribar, J.W. Lee, S. Chen, S. He, Rapid fabrication of complex 3D extracellular microenvironments by dynamic optical projection stereolithography, Adv. Mater. 24 (2012) 4266–4270.
[65] X. Chen, H.O.T. Ware, E. Baker, W. Chu, J. Hu, C. Sun, The development of an all-polymer-based piezoelectric photocurable resin for additive manufacturing, Proc. CIRP 65 (2017) 157.
[66] P. Ueberschlag, PVDF piezoelectric polymer, Sens. Rev. 21 (2001) 118–126.
[67] X. Zhou, K. Parida, O. Halevi, S. Magdassi, P.S. Lee, All 3D printed stretchable piezoelectric nanogenerator for self-powered sensor application, Sensors 20 (2020) 6748.
[68] L. Wang, K. Wang, S. Shi, N. Wang, L. Zhang, B. Lu, 3D printed 0–3 type piezoelectric composites with high voltage sensitivity, Ceram. Int. 48 (2022) 12559–12568.
[69] J.D. Eshelby, The elastic field outside an ellipsoidal inclusion, Proc. Math. Phys. Eng. Sci. 252 (1271) (1959) 561–569.
[70] L. Wang, Y. Ma, K. Wang, Y. Ma, K. Wang, B. Lu, L. Niu, X. Li, Sensors Actuat. A. Phys. 362 (2023) 114586.
[71] K. Prashanthi, N. Miriyala, R.D. Gaikwad, W. Moussa, V.R. Rao, T. Thundat, Vibrational energy harvesting using photo-patternable piezoelectric nanocomposite cantilevers, Nano Energy 2 (5) (2013) 923–932.
[72] M. Kandpal, C. Sharan, P. Poddar, K. Prashanthi, P.R. Apte, V. Ramgopal Rao, Photopatternable nano-composite (SU-8/ZnO) thin films for piezo-electric applications, Appl. Phys. Lett. 101 (2012) 104102.
[73] B. Krishna, A. Chaturvedi, N. Mishra, K. Das, Nanomechanical characterization of SU8/ZnO nanocomposite films for applications in energy-harvesting microsystems, J. Micromech. Microeng. 28 (11) (2018) 115013.
[74] N.T. Beigh, D. Mallick, Low-cost, high-performance piezoelectric nanocomposite for mechanical energy harvesting, IEEE Sensors J. 21 (19) (2021) 21268–21276.
[75] J.M. Shaw, J.D. Gelorme, N.C. LaBianca, W.E. Conley, S.J. Holmes, Negative photoresists for optical lithography, IBM J. Res. Dev. 41 (1997) 199781–199794.
[76] H.J. Fan, W. Lee, R. Hauschild, M. Alexe, G. Le Rhun, R. Scholz, A. Dadgar, K. Nielsch, H. Kalt, A. Krost, M. Zacharias, U. Gösel, Template-assisted large-scale

ordered arrays of ZnO pillars for optical and piezoelectric applications, Small 2 (2006) 561–568.
[77] M.A. Signore, G. Malucelli, D. Duraccio, C. De Pascali, A. Fioravanti, P. Siciliano, L. Francioso, Synthesis and piezoelectric characterization of UV-curable nanocellulose/ZnO/AlN polymeric flexible films for green energy generation applications, Proceedings 56 (2020) 36.
[78] I. Payo, D. Rodriguez, J. Oliva, D. Valverde, Energy harvesting from piezoelectric paint films under biaxial strain, Mater. Struct. 29 (2020) 055008.